Correlation between magnetic interactions and giant magnetoresistance in melt-spun Co 10 Cu 90 granular alloys

A. D. C. Viegas, J. Geshev, L. S. Dorneles, J. E. Schmidt, and M. Knobel

Citation: Journal of Applied Physics **82**, 3047 (1997); doi: 10.1063/1.366164
View online: http://dx.doi.org/10.1063/1.366164
View Table of Contents: http://scitation.aip.org/content/aip/journal/jap/82/6?ver=pdfcov
Published by the AIP Publishing

Correlation between magnetic interactions and giant magnetoresistance in melt-spun $Co_{10}Cu_{90}$ granular alloys

A. D. C. Viegas,[a] J. Geshev, L. S. Dorneles, and J. E. Schmidt
Instituto de Física, Universidade Federal do Rio Grande do Sul, C.P. 15051, 91501-970, Porto Alegre, RS, Brazil

M. Knobel
Instituto de Física Gleb Wataghin, Universidade Estadual de Campinas (UNICAMP), C.P. 6165, 13083-970, Campinas, SP, Brazil

(Received 7 March 1997; accepted for publication 18 June 1997)

The effects of annealing on the structural, magnetic, and magnetotransport properties of melt-spun $Co_{10}Cu_{90}$ granular alloys were investigated. The interaction effects were studied from both remanent magnetization and magnetotransport data, using two different methods to reach the demagnetized state, ac and dc demagnetization. The analysis of the structural evolution and interaction strength between the magnetic clusters clearly shows the role of some structural parameters (particle size and density, interparticle distance) and the degree of magnetic correlation in the magnetic field response of the resistance in these inhomogeneous systems. © *1997 American Institute of Physics.* [S0021-8979(97)07118-1]

I. INTRODUCTION

Granular magnetic materials composed of nanocrystalline grains of a ferromagnetic element (such as Fe, Co or Ni) immersed in a metallic matrix (normally Cu, Ag or Au), have been extensively studied in the last few years, mainly because they display an isotropic giant magnetoresistance (GMR) effect.[1,2] Besides providing similar GMR ratios to the ones attained in some magnetic multilayers,[3] the granular solids can be easily obtained either by sputtering or by melt-spinning, and their microstructure can be significantly altered by proper annealing, allowing deeper studies about the influence of the structural parameters on the giant magnetoresistance phenomenon.[4,5] Varying the thermal treatment methods and/or conditions, a broad variety of granular structures can be created,[6] which are characterized by the particle size distribution and density. Although generally difficult to study by conventional structural analysis, the structural parameters can be obtained by detailed analysis of the magnetization curves.[7,8] In this way, one can study the evolution of the GMR ratio as a function of the annealing temperature, e.g., in order to find the optimum annealing conditions to develop materials with large magnetoresistance ratios. This kind of analysis has been performed in different systems, and in the case of CuCo alloys, the maximum GMR amplitude is obtained for thermal treatments in the range of 440–500 °C.[9–11]

Despite the enormous effort done in order to understand the basic mechanisms underlying GMR and to optimize the effect for potential applications, the complex microstructure of the samples and the consequent magnetic behavior have hindered a complete understanding of the phenomenon. Several theoretical approaches have been proposed in order to explain the GMR in granular systems, and its relationship with the materials microstructure.[12–15] Analogous to the case of metallic multilayers, the GMR effect in granular systems is thought to be related to spin-dependent scattering of conduction electrons from the magnetic regions.[16–18] Assuming that the magnetic particles are essentially superparamagnetic, a parabolic behavior of the fractional magnetoresistance as a function of the reduced magnetization M/M_s is expected.[2] However, several experimental evidences of significant deviations from the parabolic law have been observed in different systems,[19–21] indicating the existence of correlation between the magnetic moments. Recently, an analytical theory which takes explicitly into account the correlation between magnetic moments was proposed by Allia *et al.*,[22] in order to explain the observed flattening of the GMR vs M/M_s curve at low fields. The presence of correlation between the magnetic precipitates has been observed by means of independent magnetic measurements,[23,24] and even direct observation of the formation of domain structures using electron microscopy with polarization analysis.[25] From a theoretical viewpoint, the absence of translational symmetry makes the calculations more involved than the multilayer case, but realistic models on the coupling between magnetic grains begin to appear in the literature.[26,27]

An alternative approach to study interactions between magnetic entities are the so-called field dependent remanence curves,[28–30] mainly used to investigate particulate recording media. A technique based on these curves, δM plot,[30] has been extensively used recently, because it proved to be very sensitive to small changes in the remanence produced by interactions between the magnetic regions of the system. However, the shape of the interaction plots depends on the initial demagnetizing procedure. An attempt to use the δM plot technique to study the correlation between the interaction effects and magnetoresistance in Fe/Cr multilayers has been recently done by Parker *et al.*[31]

The purpose of the present work is to investigate the relationship between magnetoresistance and microstructure in melt-spun $Cu_{90}Co_{10}$, taking explicitly into account the influence of magnetic interactions on the magnetoresistance behavior. The structural parameters are obtained by a detailed analysis of the hysteresis loops (Section IV), whereas

[a]Electronic mail: dcviegas@if.ufrgs.br

the interaction effects are studied using both remanent magnetization and magnetotransport data (Section V). To test the reliability of the results we have used two different methods to reach the demagnetized state: ac and dc demagnetization. The definition of the new $\delta M^{\mathrm{dc}}(H)$ plot is described in Section II. The combined analysis of the structural evolution and interaction strength between magnetic clusters shown in this article clearly shows the role of some structural parameters (particle size and density, interparticle distance) and the degree of magnetic correlation in the magnetic field response of the resistance in these inhomogeneous systems.

II. DEFINITION OF THE INTERACTION PLOTS

Most of the methods for estimation of the magnetic interaction effects in particulate and thin film media with uniaxial anisotropy are based on the Wohlfarth relation[28]

$$M_d(H)=1-2M_r(H), \tag{1}$$

where $M_r(H)$ and $M_d(H)$ are the reduced remanent magnetizations [normalized by saturation remanence $M_r(\infty)$], and H is the external field. The $M_r(H)$ curve is measured on an initially demagnetized sample by applying a positive field which is then removed and the remanence M_r is measured. A larger field is then applied and the process repeated until saturation is reached. The $M_d(H)$ curve is measured by first saturating the sample in a positive field and then measuring the remanence M_d after application of progressively larger negative fields.

Henkel[29] first noted that for the case of uniaxial particles the experimental variation of $M_r(H)$ with $M_d(H)$ gave plots showing both positive and negative curvature. The noninteracting case for ac or thermal demagnetized state corresponds to a linear plot with a gradient -2. Later, a different δM plot was defined by Kelly *et al.*[30] as

$$\delta M=M_d(H)-1+2M_r(H), \tag{2}$$

where positive values of δM were attributed to interactions promoting the magnetized state, while negative values were related to interactions tending to assist magnetization reversal. This relationship is also valid for multi-domain ferromagnets if the walls interact with the same density and distribution of pinning sites on both the initial and demagnetization branches of the magnetization curve.[32]

The initial state for the acquisition of the $M_r(H)$ curve is very important in systems with interactions, as from dc, ac, or thermal demagnetized states one can obtain very different initial remanent magnetization curves (see, e.g., Ref. 33).

For the case of uniaxial anisotropy, Bissel *et al.*[34] derived a connection between the isothermal remanent magnetization curve after dc demagnetization, $M_r^{\mathrm{dc}}(H)$, and the dc demagnetization remanence curve, $M_d(H)$. The $M_r^{\mathrm{dc}}(H)$ curve is produced by cycling the sample to the negative remanence coercivity $(-H_r)$ after previous saturation, and then reducing the applied field to zero. After dc demagnetization the particles with switching fields $<H_r$ are reversed, while those requiring fields $\geqslant H_r$ remain magnetized in the direction of the original saturation remanence. Thus, the dc remagnetization process consists of changing the direction of magnetization of the particles with small switching fields having a direction opposite to that of the magnetizing field. The resulting connections are:

$$M_r^{\mathrm{dc}}(H)=1-M_d(H) \tag{3}$$

for $H<H_r$, and

$$M_r^{\mathrm{dc}}(H)=1 \tag{4}$$

for $H\geqslant H_r$.

Here we introduce a new plot, $\delta M^{\mathrm{dc}}(H)$, defined as

$$\delta M^{\mathrm{dc}}(H)=M_r^{\mathrm{dc}}(H)-1+M_d(H) \tag{5}$$

for $H<H_r$, and

$$\delta M^{\mathrm{dc}}(H)=M_r^{\mathrm{dc}}(H)-1 \tag{6}$$

for $H\geqslant H_r$.

In the case of no interactions (and uniaxial anisotropy) $\delta M^{\mathrm{dc}}(H)$ is zero for all values of the applied field H. The corresponding Henkel plot is a straight line with a slope -1.

III. EXPERIMENTAL DETAILS

A rapidly quenched $Co_{10}Cu_{90}$ ribbon was prepared by melt-spinning in He atmosphere on a CuZr wheel.[10] The samples were submitted to furnace annealing under argon atmosphere at annealing temperatures (T_{ann}) in the 200–700 °C range for 1 h.

The resistance, R, was measured at room temperature by using the standard four-contact method. The magnetic field was applied in the ribbon's plane (there is no planar anisotropy for all of the samples). The relative GMR ratio is defined as $\Delta R/R(H)\equiv\{[R(H=0)-R(H)]/R(H=0)\}\times 100$. The maximum experimental ratio is given by $\Delta R/R(H_{\mathrm{max}})$, where $H_{\mathrm{max}}=60$ kOe is the maximum applied field.

The initial magnetization curves, hysteresis loops, as well as remanent magnetization curves were measured using an alternating gradient magnetometer at room temperature, and calibrated to the corresponding 8 kOe external field vibrating-sample magnetometer (VSM) magnetization.

The x-ray diffraction (XRD) data for the as-quenched samples are published elsewhere.[10] They show presence of Co atoms dissolved in the Cu matrix, as well as small fcc Co particles. These particles cannot be characterized by conventional XRD due to high lattice coherency between the Co particles and Cu-rich matrix, as well as the relatively small size of the particles. There is no indication of hcp Co structure. During annealing, the formation of the Co particles due to the atom diffusion process (which steadily separates the Co atoms from the Cu fcc matrix as the annealing temperature is increased) is observed.

Although difficult to study using conventional characterization techniques, further information about the microstructure can be inferred from magnetic measurements, as will be shown in Section IV.

IV. ANALYSIS OF THE MAGNETIZATION CURVES

In Fig. 1(a) are displayed the demagnetization curves for several samples annealed at different temperatures, as well as the curve for the as-quenched sample. It can be seen that,

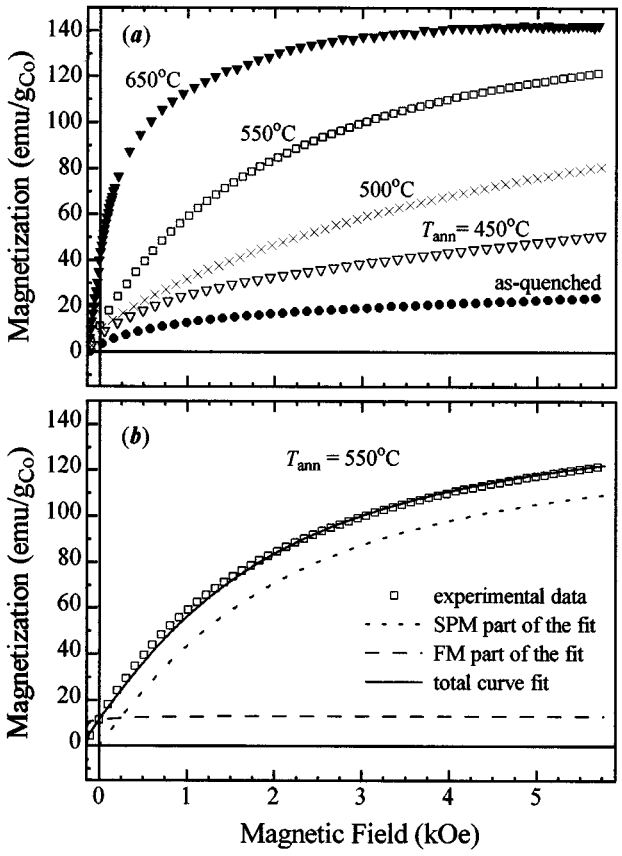

FIG. 1. (a) Magnetization vs applied field for $Co_{10}Cu_{90}$ ribbons for different annealing temperature, in units of emu per gram of Co. (b) Experimental data and fitting curves for a representative sample annealed at 550 °C.

especially for lower $T_{\rm ann}$, the samples are not saturated, and the shape of the magnetization curves is characteristic of an assembly of very small particles that exhibit superparamagnetism (SPM)—at sufficiently high temperature, the magnetization vectors of these particles are thermally agitated over their potential barriers, permitting them to rotate around their equilibrium directions. Such particles are referred to as ''unblocked'' or superparamagnetic particles.

However, all the curves show remanent magnetization M_r and coercivity H_c greater than zero. In a system consisting of SPM particles only, the existence of hysteresis could be explained by the presence of ferromagnetic interparticle interactions. As the remanence reaches a relatively large value (up to $0.25M_s$) for the samples annealed at the highest $T_{\rm ann}$, we consider our samples as consisting of two magnetic Co phases embedded in the Cu matrix: (i) noninteracting SPM particles and (ii) ''blocked'' (interacting and/or larger ferromagnetic) grains, which we will call FM entities.

The average size (D) of the SPM particles and the saturation magnetization can be obtained by fitting the experimental hysteresis loops taking into account both FM and SPM contributions.[35] The magnetization $M(H)$ of our samples can be written as

$$M(H)=M^{\rm FM}(H)+M^{\rm SPM}(H). \tag{7}$$

The term $M^{\rm FM}(H)$ gives the ferromagnetic fraction of the Co particles, which are assumed to have cubic magnetocrystalline anisotropy with four easy magnetization axes (fcc structure). For our samples, magnetic fields higher than 4 kOe are enough to saturate the FM fraction and hence the first term equals its saturation value $M_s^{\rm FM}$ independent of H. Here it is accepted that $M_s^{\rm FM}=M_r/0.866$, which holds for disordered systems of single-domain cubic anisotropy particles with four easy magnetization axes (negative first-order anisotropy constant K_1).[36] Thus, for $H>4$ kOe,

$$M^{\rm SPM}(H)=M(H)-M_s^{\rm FM}. \tag{8}$$

Under the assumption of weak interactions between the SPM particles, the magnetization of a superparamagnetic system with uniform particle size can be described by the Langevin equation $L(\alpha)=\coth(\alpha)-1/\alpha$. In real granular systems it is necessary to consider a distribution of the particle sizes. Therefore, the $M^{\rm SPM}(H)$ term should be described by a weighted superposition of Langevin functions

$$M^{\rm SPM}=M_s^{\rm Co}\int_0^\infty L\left(\frac{\mu H}{k_{\rm B}T}\right)f(V)dV, \tag{9}$$

where $\mu=M_s^{\rm Co}V$ is the magnetic moment of a single-domain Co particle with saturation magnetization $M_s^{\rm Co}$ and volume V, and $f(V)$ is the particle size distribution. Assuming spherical particles of diameter D for simplicity, a log-normal particle size distribution with width σ

$$f(D)=\frac{1}{\sqrt{2\pi}\ln\sigma}\exp\left(-\frac{(\ln D-\ln\overline{D})^2}{2(\ln\sigma)^2}\right) \tag{10}$$

is often used,[37] where $V=\pi D^3/6$. Assuming $M_s^{\rm Co}=164.8$ emu/g for the pure fcc Co,[38] we fitted the $M^{\rm SPM}(H)$ [Eq. (8)] to Eq. (9); thus, $f(D)$ and σ (usually $\sigma\approx1.0$) can be obtained.

Once $M^{\rm SPM}(H)$ is obtained, the ferromagnetic part of the experimental magnetization curve can be fitted. Assuming that the FM particles are large enough so the magnetization reversals (which occur due to a combination of thermal and field induced effects) can be neglected, one can use the model curve for a disordered fine particle system with four easy magnetization axes, $M^{\rm FM}/M_s^{\rm FM}=f[H/(2M_s^{\rm FM}/|K_1|)]$.[39] Along with M_r, it is sufficient to know just one more parameter of this curve, the coercivity $H_c^{\rm FM}$, obtained from the curve $M(H)-M^{\rm SPM}(H)$.

Thus, the total fitting demagnetization curve is made by a superposition of both SPM and FM fitting functions. These curves along with the experimental data are shown in Fig. 1(b) for one representative sample ($T_{\rm ann}=550$ °C). The agreement between theory and experiment is evident from Fig. 1(b), even in the low-field region.

Owing to the low values of the remanence of the samples annealed at lower temperatures, the type of the used FM fitting function does not change significantly the values of D and M_s. This type of analysis of magnetization curves can bring up additional information about the crystallographic structure of the magnetic phase, as the shapes of the fitting magnetization functions for the cases of one (hcp Co) or four (fcc Co) easy magnetization directions are quite dif-

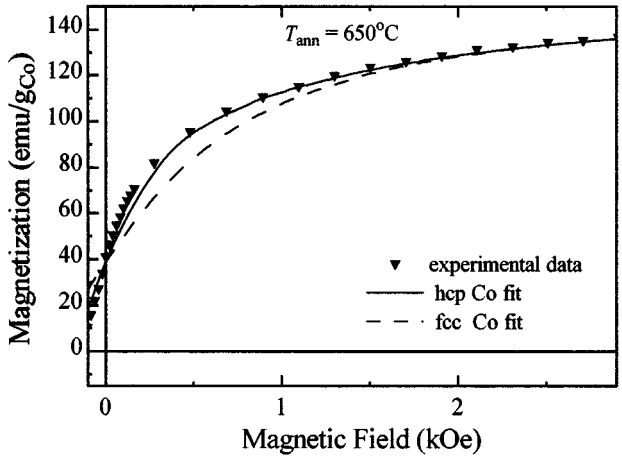

FIG. 2. Magnetization vs applied field for a $Co_{10}Cu_{90}$ ribbon annealed at 650 °C, in units of emu per gram of Co. Solid and dashed lines are the fitting curves for the cases of uniaxial (hcp) and cubic (fcc) anisotropy FM Co particles, respectively.

ferent. The low-field fittings of the magnetization curve of the sample annealed at 650 °C are shown in Fig. 2. We tried to fit the experimental data using Eq. (8) and considering the cases of hcp or fcc Co. As can be seen from Fig. 2, the uniaxial anisotropy fit is much better than the one for the case of cubic anisotropy Co particles for this annealing temperature. The present model, however, does not account for the effects of a distribution of FM particle sizes which is the situation generally observed in real systems. More precise studies should consider the sequences of thermally activated magnetization reversal and adopt certain distribution of FM particle sizes, as it is reported by Chantrell *et al.*[40] for the case of uniaxial systems, and by Walker *et al.*[41] for the case of non-interacting single-domain particles with cubic magnetocrystalline anisotropy.

V. RESULTS AND DISCUSSION

In Fig. 3, we summarize the behavior of the magnetic properties on the samples submitted to different thermal treatments. The saturation magnetization M_s and the average SPM particle size D, obtained from the fitting procedure described above, are shown in Figs. 3(a) and 3(b), along with the experimentally measured remanence M_r, coercivity H_c and remanent coercivity H_r [Figs. 3(c)–3(e)].

The magnetic field dependencies of the magnetoresistance ratios, $\Delta R/R(H)$, for several annealing temperatures are shown in Fig. 4. Except for the sample annealed at 550 °C, all the curves display a nonsaturating behavior for high field values.

As stated above, deviations from the quadratic dependence of $\Delta R/R$ on $m=M^{\mathrm{SPM}}/M_s^{\mathrm{SPM}}$ in the low-field region are often mentioned as a proof of the existence of magnetic interactions among particle; M_s^{SPM} is the superparamagnetic saturation magnetization as determined from the fit. Here, in order to estimate the interaction strength in our samples, we used the form of the reduced GMR as defined in Eq. (10) in Ref. 22

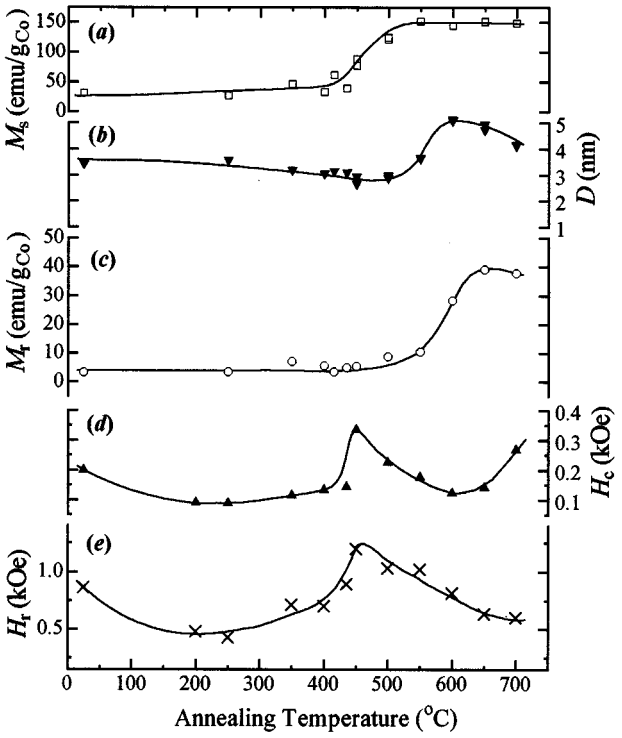

FIG. 3. Magnetic properties on the samples vs T_{ann}. (a) Saturation magnetization M_s and (b) average SPM particle size D, obtained from the fit. (c)–(e) Experimentally measured saturation remanence M_r, coercivity H_c and remanent coercivity H_r. Solid lines: guide to the eye.

$$\left(\frac{\Delta R}{R}\right)_{\mathrm{red}}=\frac{\dfrac{\Delta R}{R}-a+b}{b}. \tag{11}$$

The quantities a, b are obtained by fitting the tails at large m of the $\Delta R/R$ curves to a parabola of the type $f(m)=a-bm^2$. In the absence of correlation, $\Delta R/R_{\mathrm{red}}$ should behave as $1-m^2$. Otherwise, it should flatten out around $m=0$.[22] In Fig. 5, these reduced GMR ratios are pre-

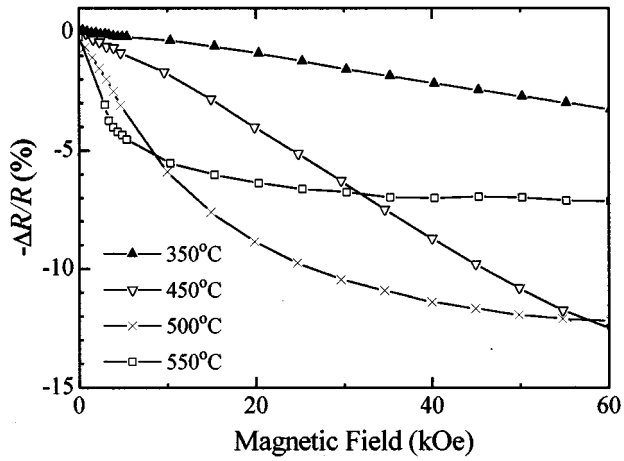

FIG. 4. Magnetic field dependencies of $\Delta R/R$ for several annealing temperatures. The lines are guide to the eye.

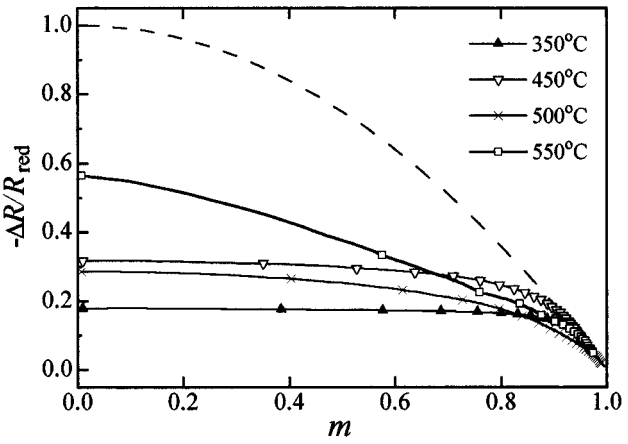

FIG. 5. Reduced $\Delta R/R_{\rm red}$ as functions of $m=M^{\rm SPM}/M_s^{\rm SPM}$ for four selected samples. The dashed line is the parabolic behavior predicted for the noninteracting case, and the solid ones are guide to the eye.

sented for four selected samples as functions of m. The dashed line is the parabolic behavior predicted for the system of randomly distributed magnetic moments.[2,42] The observed deviations are larger than those observed by Allia *et al.*[22] for samples of the same composition, which can be attributed to the larger maximum magnetic field used here. Nevertheless, as stated earlier (see Fig. 4), the magnetoresistance continues to decrease above the field at which the FM fraction is saturated, producing the long tails in the magnetoresistance curves. We conclude that because of the lack of saturation in the magnetoresistance curves for our samples, it is very difficult to use the curves in Fig. 5 for estimation of the interaction strength in melt-spun $Co_{10}Cu_{90}$ granular alloys.

Here, the magnetic interaction effects have been studied using both $\delta M^{\rm ac}$ and $\delta M^{\rm dc}$ plots, constructed from the remanent magnetization curves. The Henkel plots [$M_d(H)$ vs $M_r(H)$] obtained from the thermal, ac and dc demagnetized states for the as-quenched sample are presented in Fig. 6(a). All the plots show negative deviations from the noninteracting (for the case of uniaxial anisotropy) straight lines, dashed for the dc demagnetized state and solid for the ac and thermal demagnetization. The corresponding δM plots are shown in Fig. 6(b). There is only one minimum in each plot, and it holds for all the samples studied.

It must be noted that the Henkel-type plot, calculated for the case of non-interacting particles with four easy magnetization axes,[43] is nonlinear in a ''positive'' sense with the curve concave downwards, so the corresponding δM plot will show a positive peak. Thus, in the case of cubic anisotropy, negative values of δM indicate negative interactions as well. However, as the contributions of fcc and hcp Co phases (if co-exist, at least in our samples annealed at higher temperatures) cannot be separated, to estimate the change of the strength of the interactions as a function of $T_{\rm ann}$ we used the amplitude of the minima of the δM (ac and dc) plots. Any change of these values is attributed to the change of the relative strength of the interactions, which may be both RKKY and/or dipolar in nature, leading to complex magnetic behavior.

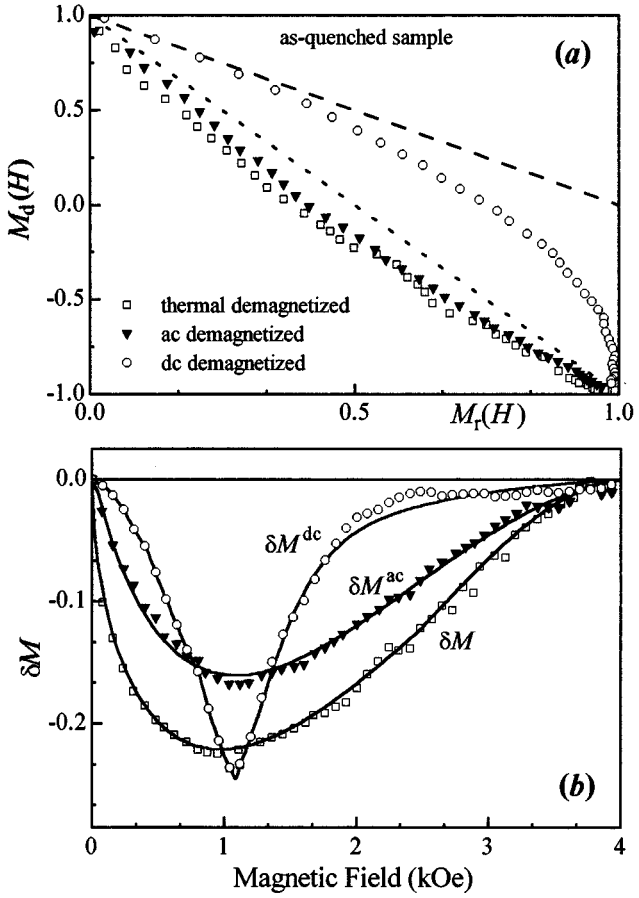

FIG. 6. (a) Representative Henkel plots obtained from the thermal, ac and dc demagnetized states for the as-quenched sample; the dotted line represents the case of no interactions (for uniaxial anisotropy) for the ac and thermal demagnetization, and the dashed one for the dc demagnetization. (b) The corresponding δM, $\delta M^{\rm ac}$, and $\delta M^{\rm dc}$ plots; the solid lines are guide to the eye.

The amplitudes of the $\delta M^{\rm dc}$ and $\delta M^{\rm ac}$ plots versus the annealing temperature are represented in Fig. 7(a). In order to compare the variations in the magnetic interactions to the changes in the magnetotransport properties of the samples, in Fig. 7(b) we plot the dependence of GMR as a function of $T_{\rm ann}$.

Our interpretation of the data follows the same approach of previous works[9,10,37] but, based on our new information, we are able to detail the different processes that occur inside the material as one anneals it. From Fig. 3 and Fig. 7, one can see that there are at least four $T_{\rm ann}$ intervals in which distinct physical transformation of the sample takes place.

(i) $T_{\rm ann}<420$ °C: in this interval, most of the parameters change slowly only with $T_{\rm ann}$, exception made for the GMR, that rapidly increases starting from $T_{\rm ann}\geqslant 350$ °C. Since GMR depends on the SPM grain size and on the distance between these grains, we can say that the system evolves in such a way as to produce new SPM particles (initially of size smaller than the average of the existent ones in the as-quenched sample) at the expense of the atomically diluted Co.[22] This would account for the slight increase of M_s and the reduction of the average SPM particle size, as seen in

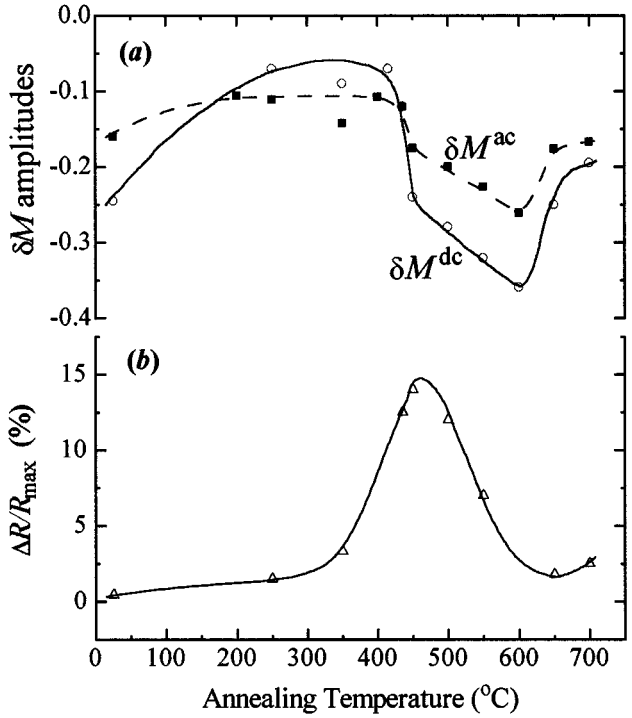

FIG. 7. (a) δM^{dc} and δM^{ac} amplitudes and (b) $\Delta R/R_{max}$ vs T_{ann}. The lines are guide to the eye.

Fig. 3. The GMR is enhanced based on the fact that D and/or the mean distance between the SPM particles approximate to their optima (for magnetoresistance) values. The mean distance, which could be reduced due to the larger number of particles present, would become comparable to the mean free path (mfp) and more selective scattering would occur.

The suggestion that only SPM particles are formed is also supported by the absence of increase of M_r, in spite of the increase of M_s. H_c and H_r increase as well, showing that the particle magnetization rotations become more collective. However, this change of the interaction behavior does not affect the δM plot amplitudes, as the interactions are approximately the same during initial magnetization and demagnetization processes.

The values H_c, H_r, and δM plot amplitudes for the annealed samples in this temperature range are smaller than the ones for the as-quenched sample. A simple explanation for this fact can be the removal of the strains (introduced by the melt-spinning) during annealing.

(ii) 420 °C$<T_{ann}<$520 °C: after the system reaches the conditions for the GMR to attain its best response (GMR reaches its maximum around 450 °C), we notice that for higher T_{ann}, there is the setup of stronger interactions between Co clusters (a rapid increase of H_r and H_c, and higher negative δM values), causing GMR to be reduced significantly. We also observe a more enhanced consumption of atomically diluted Co (represented by the increase of M_s), creating still larger number of small sized SPM particles (almost constant M_r and D continuing to decrease slowly), that now are so large in number they promote interactions between them due to the shorter distances produced therein.

Thus, annealing at temperatures higher than 450 °C causes decrease in GMR for two reasons: (1) decrease of the distances between the particles (that become of the order of the mfp); (2) appearance of ferromagnetic coupling between neighboring Co particles. Because of these couplings, the random alignment of the magnetizations of the magnetic precipitates is lost in a length scale larger than the mfp.

The fraction of FM particles in the material (represented by M_r) is not significantly altered.

(iii) 520 °C$<T_{ann}<$600 °C: for samples, annealed at T_{ann} higher than 520 °C, the process of back-diffusion of Co atoms from the Cu-matrix and formation of new Co grains is finished, indicated by the fact that M_s has reached its final value. As can be seen from the shape of the magnetization curves in Fig. 1, the average size of the SPM particles increases because they coalesce in this T_{ann} range, and some of them become large enough to be ferromagnetic, resulting in an increase of M_r. Probably, the already existing FM particles become too large compared with the mfp of the conduction electrons and/or the interactions between the SPM particles become stronger. For these FM particles, the optimal single-domain size is overcome, and the coercivities H_c and H_r consequently decrease. An increase of the strength of the magnetic interactions is observed from the further increase of the δM amplitudes (negative); consequently, GMR is reduced even more.

(iv) 600 °C$<T_{ann}<$700 °C: the samples annealed at these temperatures become much more ferromagneticlike, as can be seen from the additional increase of M_r (increase of the volume fraction of material, capable of retaining its magnetization). From the decrease of D one can conclude that (up to $T_{ann}=650$ °C, where M_r reaches a flat maximum) most of the larger SPM particles coalesce. The further decrease of D does not affect significantly M_r, as the number of remaining SPM particles is too small: those particles, that become FM, are few in number, and do not increase the remanence substantially to be observed. The reduction of M_r and to a lesser extent of M_s (Fig. 1), also observed by other workers,[6,9,22,44] may indicate that some cobalt is redissolved in the copper matrix, according to a mechanism proposed by Wecker *et al.*[9] and expected to be present at high temperatures. Other contributions to the decrease of the saturation remanence can be transition from fcc to hcp Co, observed by van Alphen and de Jonge[45] for higher annealing temperatures in Co–Ag multilayer/granular structures, appearance of elongated fcc Co particles,[46] or it may be also related to the change of interface roughness.[6] The fcc–hcp transition in the samples annealed at 650 °C and 700 °C is supported by the better low-field fitting of their magnetization curves using uniaxial instead of cubic anisotropy FM contribution (Fig. 2).

The increase of H_c in this annealing temperature range ($T_{ann}>600$ °C) can be associated to a reduction of the interactions [Fig. 7(a)], or more probably, to the final SPM–FM particle transformation, indicated by the increase of M_r. This phase transformation does not lead to increase of H_r, which does not depend on the volume fraction of FM material, but on its intrinsic properties only (saturation magnetization, anisotropy constants, etc).

VI. CONCLUSION

The detailed measurements of the complete hysteresis of annealed melt-spun $Co_{10}Cu_{90}$ granular alloys and the evaluation of the properties; therein enabled us to describe the evolution of the morphological structure of the material and relate it to the behavior of the GMR.

It is demonstrated that besides giving the average size of the SPM particles and the saturation magnetization, the fit of the experimental hysteresis loops taking into account both FM and SPM contributions (and especially the low-field magnetization region) can give additional information about the crystallographic structure of the magnetic phase.

The lack of saturation in the magnetoresistance curves for our samples does not allow the use of the deviation from the theoretical quadratic law of the reduced magnetoresistance dependence on the square of the reduced magnetization to estimate the interparticle interaction strength. Here it was done by using another technique for estimation of the interaction effects, that of δM plots, for two cases of initial demagnetization, ac and dc demagnetized states.

The analysis of the structural evolution and interaction strength between the magnetic clusters clearly shows the influence of some structural parameters as particle size and density, interparticle distance, and the degree of magnetic correlation on the magnetic field response of the resistance in these inhomogeneous systems.

ACKNOWLEDGMENTS

This work was supported by Conselho Nacional de Desenvolvimento Científico e Tecnológico (CNPq, Brazil), Fundação de Amparo à Pesquisa do Estado do Rio Grande do Sul (FAPERGS, Brazil), and Financiadora de Estudos e Projetos (FINEP, Brazil). The authors wish to thank the people from IEN ''Galileo Ferraris,'' Torino, Italy, for kindly supplying the melt-spun ribbons and for the continuous help in the development of this work. They also thank Dr. R. W. Chantrell, Dr. G. Bertotti, and Dr. R. M. Roshko for useful discussions, as well as A. Morrone for his valuable technical assistance.

[1] A. E. Berkowitz, J. R. Mitchell, M. J. Carey, A. P. Young, S. Zhang, F. E. Spada, F. T. Parker, A. Hutten, and G. Thomas, Phys. Rev. Lett. **68**, 3745 (1992).
[2] Q. Xiao, J. S. Jiang, and C. L. Chien, Phys. Rev. Lett. **68**, 3749 (1992).
[3] M. N. Baibich, J. M. Broto, A. Fert, F. Nguyen Van Dau, F. Petroff, P. Etienne, G. Creuzet, A. Friederich, and J. Chazelas, Phys. Lett. B **61**, 2472 (1988).
[4] J.-Q. Wang and G. Xiao, Phys. Rev. B **49**, 3982 (1994).
[5] B. Dieny, S. R. Teixeira, B. Rodmacq, C. Cowache, S. Auffret, O. Redon, and J. Pierre, J. Magn. Magn. Mater. **130**, 197 (1994).
[6] R. H. Yu, X. X. Zhang, J. Tejada, J. Zhu, M. Knobel, P. Tiberto, and P. Allia, J. Appl. Phys. **78**, 5062 (1995).
[7] R. Von Helmolt, J. Wecker, and K. Samwer, Phys. Status Solidi B **182**, K25 (1994).
[8] P. Allia, F. Ghigo, M. Knobel, P. Tiberto, and F. Vinai, J. Magn. Magn. Mater. **157/158**, 319 (1996).
[9] J. Wecker, R. von Helmolt, L. Schultz, and K. Samwer, IEEE Trans. Magn. **29**, 3087 (1993).
[10] R. H. Yu, X. X. Zhang, J. Tejada, M. Knobel, P. Tiberto, and P. Allia, J. Appl. Phys. **78**, 392 (1995).
[11] B. Dieny, A. Chamberod, J. B. Genin, B. Rodmacq, S. R. Teixeira, S. Auffret, P. Gerald, O. Redon, J. Pierre, R. Ferrer, and B. Barbara, J. Magn. Magn. Mater. **126**, 433 (1996).
[12] M. Rubinstein, Phys. Rev. B **50**, 3830 (1994).
[13] Y. Asano, A. Oguri, J. Inoue, and S. Maekawa, Phys. Rev. B **49**, 12 831 (1994).
[14] J. H. Kim, J. Q. Xiao, C. L. Chien, and Z. Tesanovic, Solid State Commun. **89**, 157 (1994).
[15] L. Sheng, Z. D. Wang, D. Y. Xing, and J.-X. Zhu, Phys. Rev. B **53**, 8203 (1996).
[16] S. Zhang, Appl. Phys. Lett. **61**, 1855 (1992).
[17] S. Zhang and P. M. Levy, J. Appl. Phys. **73**, 5315 (1993).
[18] T. A. Rabedeau, M. F. Toney, R. F. Marks, S. S. P. Parkin, R. F. C. Farrow, and G. R. Harp, Phys. Rev. B **48**, 16 810 (1993).
[19] B. J. Hickey, M. A. Howson, S. O. Musa, and N. Wiser, Phys. Rev. B **51**, 667 (1995).
[20] J. F. Gregg, S. M. Thompson, S. J. Dawson, K. Ounadjela, C. R. Staddon, J. Hamman, C. Fermon, G. Saux, and K. O'Grady, Phys. Rev. B **49**, 1064 (1994).
[21] M. El-Hilo, K. O'Grady, and R. W. Chantrell, J. Appl. Phys. **76**, 6811 (1994).
[22] P. Allia, M. Knobel, P. Tiberto, and F. Vinai, Phys. Rev. B **52**, 15 398 (1995).
[23] C. Bellouard, B. George, and G. Marchal, J. Phys.: Condens. Matter **6**, 7239 (1994).
[24] H. J. Blythe and V. M. Fedosyuk, J. Phys.: Condens. Matter **7**, 3461 (1995).
[25] A. Gavrin, M. H. Kelley, J. Q. Xiao, and C. L. Chien, Appl. Phys. Lett. **66**, 1683 (1995).
[26] D. Altbir, J. d'Albuquerque e Castro, and P. Vargas, Phys. Rev. B **54**, 6823 (1996).
[27] P. Allia, P. Tiberto, and F. Vinai, J. Appl. Phys. **81**, 4599 (1997).
[28] E. P. Wohlfarth, J. Appl. Phys. **29**, 595 (1958).
[29] O. Henkel, Phys. Status Solidi B **7**, 919 (1964).
[30] P. E. Kelly, K. O'Grady, P. I. Mayo, and R. W. Chantrell, IEEE Trans. Magn. **25**, 3881 (1989).
[31] M. R. Parker, D. Seale, E. Tsang, J. A. Barnard, S. Hossain, D. A. Richards, and M. L. Watson, J. Appl. Phys. **73**, 6408 (1993).
[32] R. A. McCurie and P. Gaunt, in Proceedings of the International Conference on Magnetism, Nottingham, 1964, p. 780 (unpublished).
[33] M. Fearon, R. W. Chantrell, and E. P. Wohlfarth, J. Magn. Magn. Mater. **86**, 197 (1990).
[34] P. Bissel, R. Chantrell, G. Tomka, J. Knowles, and M. Sharrock, IEEE Trans. Magn. **25**, 3650 (1989).
[35] B. J. Hickey, M. A. Howson, S. O. Musa, G. J. Tomka B. D. Rainford, and N. Wiser, J. Magn. Magn. Mater. **147**, 253 (1995).
[36] R. Gans, Ann. Phys. **15**, 28 (1932).
[37] R. H. Yu, X. X. Zhang, J. Tejada, J. Zhu, and M. Knobel, J. Appl. Phys. **79**, 1979 (1996).
[38] L. J. Swartzendruber, J. Magn. Magn. Mater. **100**, 573 (1991).
[39] J. Geshev, O. Popov, V. Masheva, and M. Mikhov, J. Magn. Magn. Mater. **92**, 185 (1990).
[40] R. W. Chantrell, K. O'Grady, A. Bradbury, S. W. Charles, and J. Popplewell, J. Phys. D **18**, 2505 (1985).
[41] M. Walker, P. I. Mayo, K. O'Grady, S. W. Charles, and R. W. Chantrell, J. Phys.: Condens. Matter **5**, 2779 (1993).
[42] Q. Xiao, J. S. Jiang, and C. L. Chien, Phys. Rev. B **46**, 9266 (1992).
[43] J. Geshev and M. Mikhov, J. Magn. Magn. Mater. **104–107**, 1569 (1992).
[44] J. R. Childress and C. L. Chien, J. Appl. Phys. **70**, 5885 (1991).
[45] E. A. M. van Alphen and W. J. M. de Jonge, Phys. Rev. B **51**, 8182 (1995).
[46] A. Hütten and G. Thomas, Ultramicroscopy **52**, 581 (1993).